PERGAMON

Solid-State Electronics 45 (2001) 143–148

SOLID-STATE ELECTRONICS

Extraction of Schottky diode parameters with a bias dependent barrier height

V. Mikhelashvili, G. Eisenstein *, R. Uzdin

Department of Electrical Engineering, Technion, Haifa 32000, Israel

Received 14 August 2000; received in revised form 21 October 2000; accepted 25 October 2000

Abstract

We describe a technique to extract device parameters of a Schottky barrier diode whose barrier height is bias dependent and which contains a linear series resistance. The extracted parameters include the saturation current (zero bias barrier height), the voltage dependence of the barrier height and of the ideality factor as well as series resistance. The technique makes use of forward biased current–voltage (I–V) characteristic and voltage-dependent differential slope curve $\alpha = \mathrm{d}(\ln I)/\mathrm{d}(\ln V)$. The method is verified using simulated and experimental I–V curves of an Al–pSi structure. The proposed procedure is not limited to Schottky barrier diodes but may be applied to other diode types based on P–N junction. © 2001 Elsevier Science Ltd. All rights reserved.

1. Introduction

The deviation from ideality of metal–semiconductor structure (M–S) current–voltage (I–V) characteristics is related to variation of barrier height with applied voltage [1,2]. An ideality factor, $\beta > 1$, is commonly used to phenomenologically model the non-ideal characteristics (with $\beta = 1$ for the pure thermionic emission case). Values of β different from unity result from image forces acting on the barrier height (Φ_B) and interface states or traps, localized in the unavoidable native oxide covering the semiconductor, which are populated or released with applied voltage thereby modifying the effective Φ_B. At moderate bias levels, the main reason for the deviation from a pure exponential characteristics is the fact that various carrier transport mechanisms such as tunneling through a barrier and generation–recombination current in the depletion region occur simultaneously with thermionic emission thereby changing β [1,2]. In the high voltage regime, the I–V characteristics deviate from its exponential form due to the presence of a linear or nonlinear series resistance (R_S) [1].

The ability to determine the voltage dependence of β is important for establishing the exact current flow mechanisms as well as to extract correct parameters of Schottky diodes: the saturation current (I_{S0}) which gives the zero bias barrier height (Φ_{B0}) and the voltage dependence of Φ_B in the presence of R_S. Several techniques have been published [1–7], which address the $\beta(V)$ problem. Most do not consider the series resistance except for Refs. [6,7]. In Refs. [1–3] the voltage dependence of the ideality factor is established assuming, a priori, that β has a constant value. The method to determine $\beta(V)$, suggested in Refs. [4,5], includes graphical differentiation, which uses experimental I–V characteristic of an Au/GaAs Schottky diode with interface states and trapping levels placed in the native oxide of the GaAs. This technique is not only labor-consuming but does not take into account the series resistance. The graphical technique suggested by Norde [8] has been developed in Ref. [7]. It uses the Rhoderic approach [2] of linear dependence of the barrier height (that is image potential) on applied bias, which is appropriate only at low voltages when the deviation of the ideality factor from one is insignificant. The method developed in Ref. [6] stands out as the most reliable one. However it includes a cumbersome experimental procedure in which external resistors (specific for each diode) have to be added followed by complicated curve fitting. Above and beyond

* Corresponding author. Fax: +972-4-8323-041.
E-mail address: gad@ee.technion.ac.il (G. Eisenstein).

0038-1101/01/$ - see front matter © 2001 Elsevier Science Ltd. All rights reserved.
PII: S0038-1101(00)00227-6

that, the technique assumes that the ideality factor has the same value for different current levels, with and without external resistance, but this leads to different values of the voltage drop ($V_J = V - IR_S$) across the junction (see Eqs. (7) and (11) in Ref. [6]). This requirement may only be fulfilled at low voltages, when $V_J \gg IR_S$.

In this paper we propose a simple analytical method to determine the character $\beta(V)$ from measured *I–V* data and to extract the saturation current (zero bias barrier height) and the series resistance without the need to resort to complicated graphical differentiation technique [4,5], elaborate experimental procedures [6], or to the technique [7], which is valid only under limited conditions. The procedure was tested on a simulated $\beta(V)$ and experimental *I–V* characteristic of an Al–pSi structure.

The suggested technique is based on an analysis of the differential slope of the experimental *I–V* characteristics.

$$\alpha = \frac{\mathrm{d}(\ln I)}{\mathrm{d}(\ln V)} \tag{1}$$

The usefulness of transforming the experimental *I–V* characteristics in accordance with Eq. (1) was demonstrated in Refs. [9–14]. This formalism enables to trace changes in the current flow mechanisms and to extract device parameters of a single and double injection system as well as metal–semiconductor and P–N diodes whose ideality factor is voltage independent.

2. Extraction methods of the voltage dependent ideality factor

The forward *I–V* characteristic of a Schottky barrier diode whose barrier height is bias dependent for bias levels larger than $3kT/q$ is described by [1,2],

$$I = I_{S0} \exp \frac{q(V - IR_S)}{\beta(V_J)kT} \tag{2}$$

where

$$I_{S0} = SA^* T^2 \exp\left(-\frac{\Phi_{B0}}{kT}\right) \tag{3}$$

Here V, q, k, and T are the total applied voltage, the electron charge, the Boltzmann constant and the absolute temperature, respectively. The contact area is S and A^* is the Richardson constant.

The ideality factor whose only voltage dependence stems from the voltage dependence of the Schottky barrier height, is expressed by [2],

$$\beta = \frac{1}{\left(1 - \frac{\Delta\Phi_B}{V}\right)} \tag{4}$$

where $\Delta\Phi_B = \Phi_B - \Phi_{B0}$ is the change in barrier height due to the applied voltage. The establishment of the actual form of the $\beta(V)$ dependence requires solution of the differential equation

$$\frac{kT}{q}\frac{\mathrm{d}(\ln I)}{\mathrm{d}V} = \frac{1}{\beta}\left(1 - \frac{\mathrm{d}I}{\mathrm{d}V}R_S\right) - \frac{V\left(1 - \frac{IR_S}{V}\right)}{\beta^2}\frac{\mathrm{d}\beta}{\mathrm{d}V} \tag{5}$$

Note that the conventional linear approximation of $\ln(I) - V$ (see Eq. (2)) neglects the second term in the right-hand side of Eq. (5), which implies the condition $(\mathrm{d}\beta/\mathrm{d}V) = 0$ or a linear dependence of $\Delta\Phi_B$ on voltage in Eq. (4) is assumed. This formalism with the additional approximation of $R_S = 0$ was used in Refs. [1–3] to determine the voltage dependence of ideality factor of practical devices. The linear approximation of the image potential, which was assumed in Ref. [7], causes a constant value of β in accordance with Eq. (4).

3. Power exponent method

Simple algebraic manipulation of Eq. (2), using Eq. (1) yields

$$\alpha = \frac{qV}{kT}\left[\frac{1}{\beta} - \frac{(V - IR_S)}{\beta^2}\frac{\mathrm{d}\beta}{\mathrm{d}V}\right]\frac{1}{\left(1 + \frac{qIR_S}{\beta kT}\right)} \tag{6}$$

The inclusion of the $\beta(V)$ dependence according to Eq. (4) in Eq. (6) results in

$$\alpha = \frac{qV}{kT}\left[\left(1 - \frac{IR_S}{V^2}\Delta\Phi_B\right) - \left(1 - \frac{IR_S}{V}\right)\frac{\mathrm{d}\Delta\Phi_B}{\mathrm{d}V}\right] \times \frac{1}{\left[1 + \frac{qIR_S}{kT}\left(1 - \frac{\Delta\Phi_B}{V}\right)\right]} \tag{7}$$

It is seen from Eqs. (6) and (7), that in the case of pure thermionic emission the power exponent changes linearly with voltage in the $IR_S \ll V_J$ regime. It goes through a maximum at a moderate bias due to R_S and it becomes a non-linear function of the bias when $IR_S \gg V_J$ [10]. In the case of a voltage independent ideality factor, Eq. (6) permits to extract Schottky or P–N junction diodes parameters according to the techniques suggested in Ref. [10].

A solution of the differential Eq. (6) for β yields:

$$\beta = \frac{qV}{kT}\left(1 - \frac{IR_S}{V}\right)\frac{1}{\int_{V_0=3\frac{kT}{q}}^{V}\frac{\alpha}{V}\mathrm{d}V} \tag{8}$$

and using Eq. (8) in Eq. (2) we can obtain an equation to determine the saturation current and therefore the zero bias barrier height.

$$I_{S0} = \frac{I}{\exp\left[\int_{V_0=3\frac{kT}{q}}^{V}\frac{\alpha}{V}\mathrm{d}V\right]} \tag{9}$$

$$\Phi_{B0} = kT\left[\ln\left(\frac{I}{SA^*T^2}\right) - \int_{V_0=3\frac{kT}{q}}^{V} \frac{\alpha}{V}\mathrm{d}V\right] \tag{10}$$

A numerical solution of Eq. (8) gives the $\beta(V)$ dependence at low voltages when the influence of the series resistance causes a small change in the behavior of the I–V curves. However the determination of the actual nature of $\beta(V)$ in the high bias regime requires knowledge of R_S. In the high bias regime, changes in β have a negligible effect on the I–V characteristic compared to changes caused by the IR_S voltage drop. Therefore, R_S may be determined under the assumption $(\mathrm{d}\beta/\mathrm{d}V) = 0$ and this leads to [10]

$$R_S = \frac{1}{\alpha_m^2}\frac{V_m}{I_m} \tag{11}$$

$$R_S = \frac{(1-\gamma)}{\alpha^2}\frac{V}{I} \tag{12}$$

Eqs. (11) and (12) allow to extract R_S from the power exponent maximum: α_m, V_m, I_m (the maximum value of α and the bias points in which it occurs [10]) or from I–V data and the corresponding calculated α–V characteristics with the parameter

$$\gamma = \frac{\mathrm{d}(\ln\alpha)}{\mathrm{d}(\ln V)} \tag{13}$$

The limitation and accuracy of Eqs. (11) and (12) will be considered below.

4. Verification of the parameter extraction method

4.1. Calculated I–V characteristic

A $\beta(V)$ function, taken from Ref. [6], is shown in Fig. 1 (curve 1). The low voltage part of this curve was obtained by the graphical differentiation method of the experimental I–V curve of an Au/nGaAs Schottky barrier diode given in Ref. [4].

Fig. 2a shows the calculated I–V characteristics based on Eq. (2) for ($A^* = 4.4$ A/cm^{2}K^2), $\Phi_{B0} = 0.88$ eV, $S = 0.01\,\mathrm{cm}^2$ and various series resistance values taking into account the data of curve 1 in Fig. 1. The α–V transformation of these I–V characteristics is given in Fig. 2b. The first maximum is caused by a change in the current flow mechanism at low bias, which is originated by the change of barrier height with voltage (see the beginning part of the $\beta(V)$ characteristic (curve 1, Fig. 1)). The behavior of α–V at moderate voltages, when $R_S = 0$ (curve 1 of Fig. 2b), is attributed to the non-monotonic form of $\beta(V)$ at $V > 0.5$ V (see curve 1 of Fig. 1). The influence of the series resistance is seen in the second maximum, which is followed by a decrease in α (see curves 2–4 of Fig. 2b). A large R_S causes a shift of the second maximum to lower voltages while it simultaneously lowers its value. Using the α–V data in Eq. (8) gives the voltage dependent effective ideality factor $\beta'(V) = \beta(V_J)/(1 - (IR_S/V))$. The set of $\beta'(V)$ dependencies for the I–V curves of Fig. 2a are shown in Fig. 1 (curves 2–5). It can be seen that for $R_S = 0$ the calculated $\beta'(V)$ (curve 2) is very close to the initial one (curve 1). The maximum differences are less than 3% at low voltages and less than 1% at high bias levels. The addition of a series resistance changes the effective ideality factor at high voltage and the voltage in which this changes starts to be noticeable decreases as R_S increases (curves 3–5 of Fig. 1).

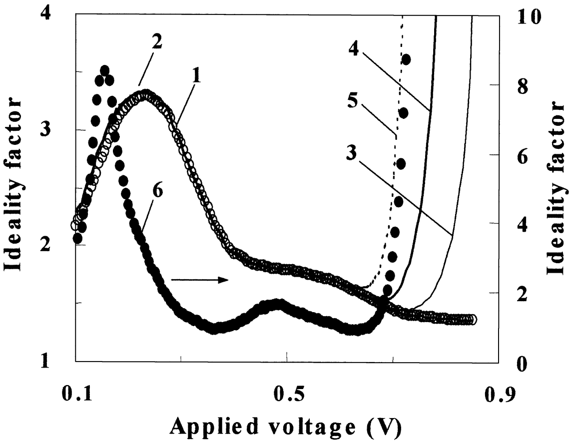

Fig. 1. Ideality factor dependence on applied voltage. Real β (curves 1 and 2), effective β (curves 3–5) and calculated β (curve 6). Curve 1 – dotted curve, calculated in accordance with Refs. [4,6]; curve 2 – solid line, calculated numerically by Eq. (8) for $R_S = 0$, utilizing the data of curve 1 in Fig. 2; curves 3–5 – solid lines, calculated numerically by Eq. (8) without taking into account the values of the series resistance (see below data of curves 2–4 in Fig. 2); curve 6 – dotted curve, calculated by Eq. (5) (for$(\mathrm{d}\beta/\mathrm{d}V)$ and $R_S = 0$), utilizing the data of curve 1 in Fig. 2.

Fig. 3 shows the change of the series resistance with voltage calculated using Eq. (12) from the data in curves 2 and 3 ($R_S = 10$ and 100 Ω). It is clear that in the voltage range including the second maximum R_S is bias independent over a large voltage range. The calculated R_S hardly differs very little from its simulated value, in particular when R_S is large. This fact is demonstrated by the dependencies of the deviation of R_S, calculated at various currents, from its true simulated value (Fig. 4). The increase in the accuracy of extraction of the series resistance requires the measurement of the I–V characteristic up to the voltage where the α–V curve is far beyond its maximum. This condition for $R_S < 10$ Ω requires a current measurement up to 5–10 mA to provide the deviation of series from true one less than 4–5% (see that of Fig. 4). The determination of R_S based on Eq.

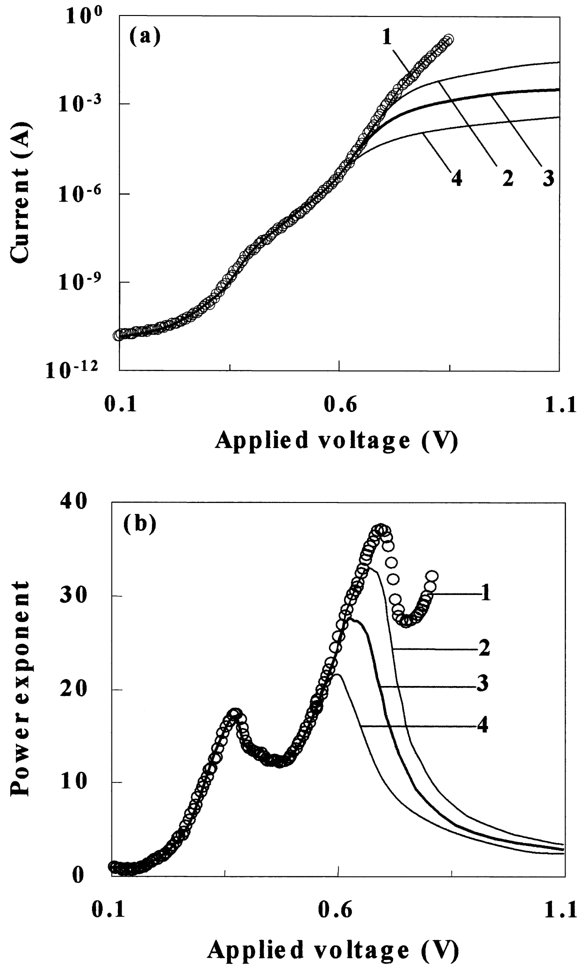

Fig. 2. (a) Calculated I–V, (b) α–V characteristics, utilizing the data of $\beta(V)$ shown in curve 1 of Fig. 1, for different series resistances: Curve 1 – $R_S = 0$, 2–10, 3–100 and 4–1000 Ω.

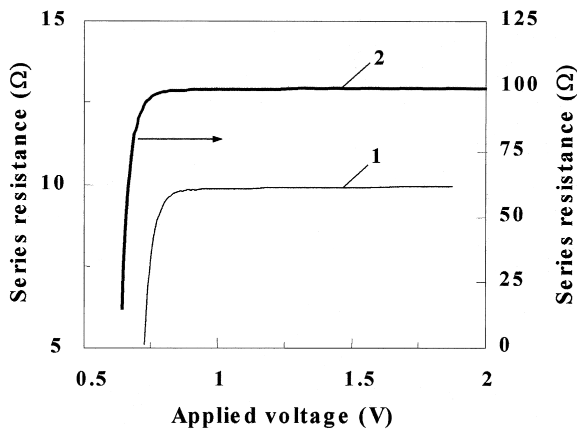

Fig. 3. Voltage dependencies of the series resistance calculated by Eq. (12), using the data of Fig. 2. Curves 1 and 2 are respectively, in accordance with the data of curves 2 and 3 in Fig. 2.

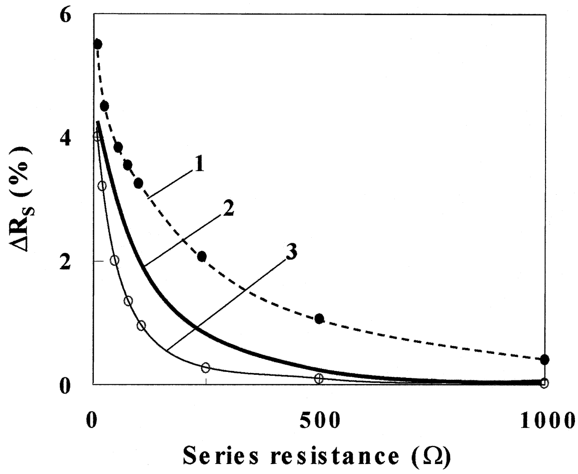

Fig. 4. The dependencies of the relative accuracy of the extracted series resistance (Eq. (12)) on the simulated resistance at different currents through the diode. Curve 1 – 5 mA, 2 – 10 mA, 3 – 20 mA.

(11) is less reliable due to influence of the strong nonlinearity in the low voltage regime of the $\beta(V)$ dependence.

Fig. 5 illustrates the influence of the series resistance deviation from its simulated value on the accuracy of the calculated ideality factor in accordance with Eq. (8). It can be seen that this issue becomes noticeable only at high voltages, where the 5% deviation in accuracy of the R_S causes a larger than 5% change in the calculated ideality factor. Note that the deviation of the ideality factor dependencies from the initially simulated one in the voltage range of interest is lower than the corresponding deviation arrived by the method suggested in Ref. [6] (see Figs. 9 and 10 in Ref. [6]).

4.2. Experimental I–V characteristic

The parameter extraction technique was applied to an Al–pSi structure with a Si resistivity of 5.7 Ωcm, measured by four probe system, and contact area of $S = 0.00028$ cm^2 ($R_S = 595$ Ω). A thin 10–15 Å native oxide film covered the Si substrate before deposition of the contact. Experimental (without smoothing [1]) room temperature I–V characteristic and the corresponding calculated α–V curves are shown in Fig. 6. The voltage dependence of the series resistance, calculated by Eq. (12) is shown in Fig. 7. We note a large voltage range where R_S is essentially unchanged with an average value

[1] In order to improve the parameter extraction accuracy, the experimental I–V, α–V and γ–V dependencies must be smoothed to avoid errors which common when high order derivatives are used.

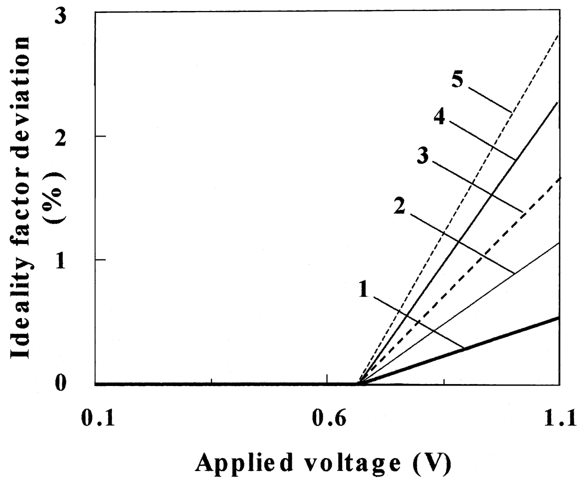

Fig. 5. Variation with applied voltage of the percent deviation of β (extracted using Eq. (8)) from true value due to the change in the relative accuracy of series resistance. Curve 1 – $\Delta R_S =$ 1%, 2 – 2%, 3 – 3%, 4 – 4%, 5 – 5%.

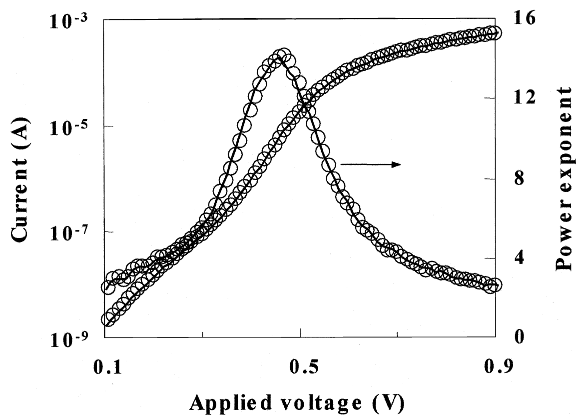

Fig. 6. Experimental (···) and calculated (—) I–V and α–V plots of an Al–pSi Schottky diode.

of $R_S = 595\ \Omega$, which is very close to the one determined from direct measurement of the resistivity.

The $\beta'(V)$ dependence calculated from Eq. (8) is shown in Fig. 8 (curve 1). Using the obtained average experimental value of R_S in Eq. (8) yields the actual $\beta(V)$ dependence as illustrated by curve 2. Also shown in Fig. 8 (curve 3) is the $\beta(V)$ dependence calculated by a conventional method [1,2] where the I–V characteristic is differentiated in accordance with Eq. (5) under the assumption of $(\mathrm{d}\beta/\mathrm{d}V)$ and $R_S = 0$. It is obvious that curves 2 and 3 differ significantly in both the low and high bias regimes. The behavior of the actual $\beta(V)$ (curve 2) at low voltage is close to the characteristic in the case of a measurable density of interface states or trap levels which penetrate into the native oxide on the

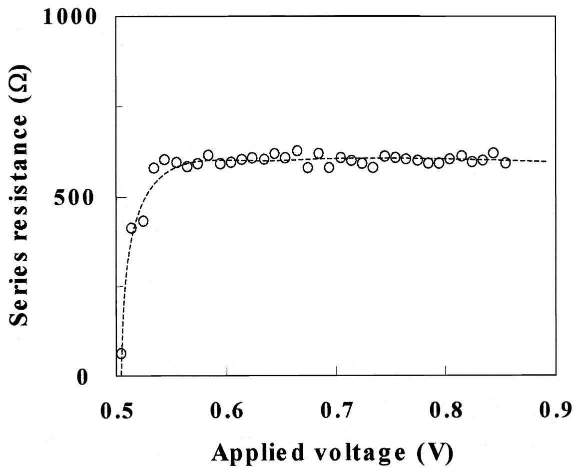

Fig. 7. Voltage dependence of the series resistance extracted by Eq. (12) using the experimental data of Fig. 6.

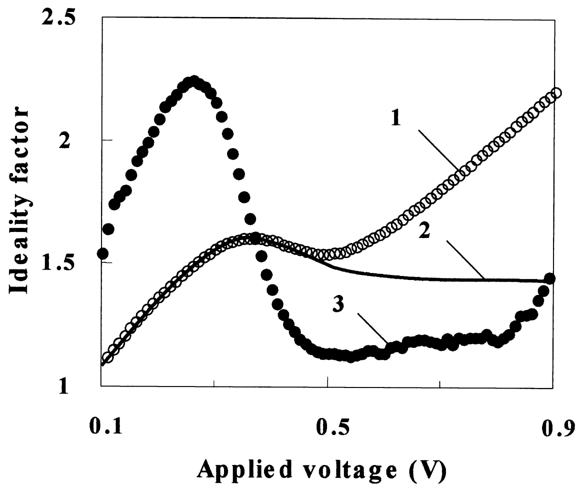

Fig. 8. Voltage dependence of the calculated ideality factors, obtained from the data of Fig. 6. Curves 1 and 2 – ideality factors extracted from Eq. (8), respectively without and with taking into account the series resistance $R_S = 595\ \Omega$. Curve 3 – calculated by Eq. (5) for $(\mathrm{d}\beta/\mathrm{d}V) = 0$ and $R_S = 595\ \Omega$.

metal–semiconductor boundary [2,15]. From the $\beta(V)$ curve in the low bias regime of curve 2 in Fig. 8 using Eq. (4) we can get the voltage dependence of $\Delta\Phi_B$ which is shown in Fig. 9. The difference from the dependence in the case where the influence of image forces on barrier height dominates ($\Delta\Phi_B \sim V^{0.25}$ [1,2], curve 1) supports the argument for the role played by the trap levels, when the variation of $\Delta\Phi_B$ with applied bias is significant [5].

The calculated saturation current (Eq. (9)) is almost constant as seen in Fig. 10. Its average value and therefore the zero bias barrier height determined by Eq. (10), are equal respectively, to $I_{S0} = 4.2 \times 10^{-11}$ A and

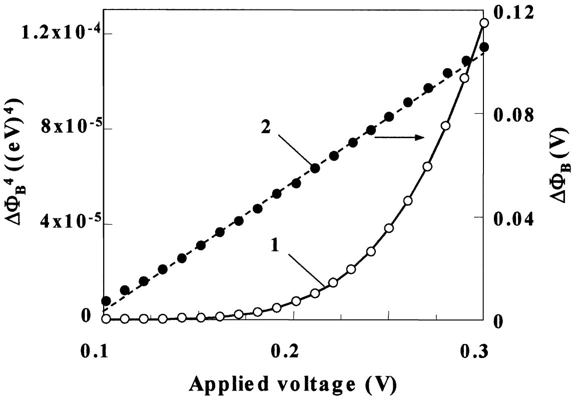

Fig. 9. $\Delta\Phi_B$ versus applied voltage. Curve 1 plotted in a scale corresponding to the influence of the image forces. Curve 2, plotted in conventional coordinates.

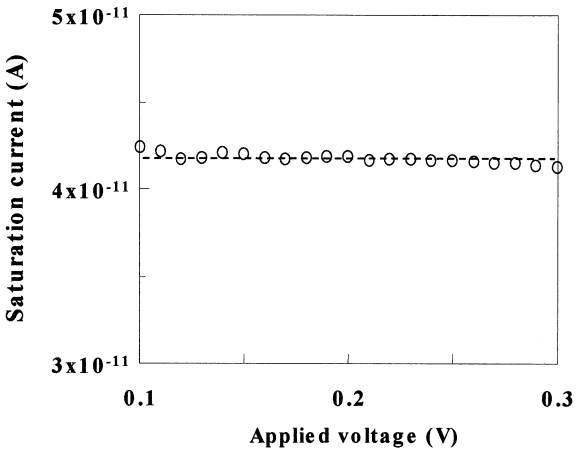

Fig. 10. Saturation current versus applied voltage. I_{S0} was calculated by Eq. (9) using the data of Fig. 6.

$\Phi_{B0} = 0.803$ eV (here the Richardson coefficient was taken as ($A^* = 120\ \mathrm{A/cm^2\,K^2}$) [1]). The determined value of Φ_{B0} differs from the value given in Ref. [1] for an Al–pSi structure (~0.58 eV), obtained for evaporated aluminum on cleaved or chemical purified silicon. When the surface or trap states exist on the metal–semiconductor boundary, the surface Fermi level is defined by these states and therefore the value of the barrier height does not depend only on the contact materials but may vary due to doping level and surface properties of the semiconductor [1]. An additional reason for the large obtained barrier height may be its inhomogeneity [2] over the contact area [16] or a variation of the physical gaps between the Si surface and the metal due to non-uniformity of the interfacial native oxide thickness [9,12, 17,18]. These occur as our Si substrate was not been etched prior to evaporation and the structure was not annealed during or after the Al deposition. It should be remarked, however, that the determination of the exact reasons, causing the observed large barrier height, requires additional study and is beyond of the scope or purpose of this paper.

[2] In the case of any inhomogeneity of the barrier height over the contact area [16], the result reflects the voltage dependence of its mean quantity.

5. Conclusion

In summary, we have described a new procedure to extract physical parameters of a Schottky barrier diode, the ideality factor of which is bias dependent and which contains a series resistance. The technique was applied to simulated as well as measured data and was found to yield accurate parameters in all cases.

References

[1] Sze SM. Physics of semiconductor devices. New York: Wiley; 1981.
[2] Rhoderic EH. Metal–semiconductor contacts. Oxford: Clarendon Press; 1978.
[3] Popescu C, Manifacier JC, Ardebili R. Phys Stat Sol (a) 1996;158:611–21.
[4] Maeda K, Ikoma H, Sato K, Ishida T. Appl Phys Lett 1993;62:2560–2.
[5] Ishida T, Ikoma H. J Appl Phys 1993;74:3977–82.
[6] Lyakas M, Zaharia R, Eizenberg M. J Appl Phys 1995;78:5481–9.
[7] McLean AB. Semicond Sci Technol 1986;1:177–9.
[8] Norde H. J Appl Phys 1979;50:5052–3.
[9] Zyuganov AN, Svechnikov SV. Injection contact phenomena in semiconductors. Kiev: Naukova Dumka; 1981 [in Russian].
[10] Mikhelashvili V, Eisenstein G, Garber V, Fainleib C, Bahir G, Ritter D, Orenstein M, Peer A. J Appl Phys 1999; 85:6873–83.
[11] Mikhelashvili V, Eisenstein G. J Appl Phys 1999;86:6965–9.
[12] Bagratishvili GD, Dzanelidze RB, Jishiashvili DA, Piskanovskii LV, Zyuganov AN, Mikhelashvili V, Smertenko PS. Phys Stat Sol (a) 1981;65:701–7.
[13] Zyuganov AN, Zorikov VV, Matinova MS, Mikhelashvili V, Chikovani RI. Sov Tech Phys Lett 1981;7:493–5.
[14] Mikhelashvili V, Betzer Y, Prudnikov I, Orenstein M, Ritter D, Eisenstein G. J Appl Phys 1998;84:6747–52.
[15] Maeda K, Umezu I, Ikoma H, Yoshimura T. J Appl Phys 1990;68:2858–67.
[16] Song YP, Van Meirhaeghe RL, Laflere WH, Cardon F. Solid-State Electron 1986;29:633–8.
[17] Pekar SI. Zh Eksper i Teoret Fiziki 1940;10:1210–24 [in Russian].
[18] Pekar SI. Zh Eksper i Teoret Fiziki 1941;11:708–16 [in Russian].